Molecular Human Reproduction, Vol.21, No.1 pp. 66–80, 2015
Advanced Access publication on September 18, 2014 doi:10.1093/molehr/gau088

molecular human reproduction

ORIGINAL RESEARCH

Primordial germ cell development in the marmoset monkey as revealed by pluripotency factor expression: suggestion of a novel model of embryonic germ cell translocation

N. Aeckerle[1], C. Drummer[1], K. Debowski[1], C. Viebahn[2], and R. Behr[1,*]

[1]Stem Cell Biology Unit, German Primate Center – Leibniz Institute for Primate Research, Kellnerweg 4, 37077 Göttingen, Germany
[2]Department of Anatomy and Embryology, Center of Anatomy, University of Göttingen, Kreuzbergring 36, 37075 Göttingen, Germany

*Correspondence address. Stem Cell Biology Unit, German Primate Center, Kellnerweg 4, 37077 Göttingen, Germany. Tel: +49-551-3851-132; Fax: +49-551–3851–431; E-mail: rbehr@dpz.eu

Submitted on January 28, 2014; resubmitted on September 5, 2014; accepted on September 15, 2014

ABSTRACT: Primordial germ cells (PGCs) are the embryonic progenitors of sperm and egg cells. Mammalian PGCs are thought to actively migrate from the yolk sac endoderm over long distances across the embryo to reach the somatic genital ridges. The general principles of mammalian PGC development were discovered in mice. In contrast, little is known about PGC development in primates due to extremely limited access to primate embryos. Here, we analyzed 12 well preserved marmoset monkey (*Callithrix jacchus*) embryos covering the phase from PGC emergence in the endoderm to the formation of the sexually differentiated gonad (embryonic day (E) 50 to E95). We show using immunohistochemistry that the pluripotency factors OCT4A and NANOG specifically mark PGCs throughout the period studied. In contrast, SALL4 and LIN28 were first expressed ubiquitously and only later down-regulated in somatic tissues. We further show, for the first time, that PGCs are located in the endoderm in E50 embryos in close spatial proximity to the prospective genital ridge, making a long-range migration of PGCs dispensable. At E65, PGCs are already present in the primitive gonad, while significantly later embryonic stages still exhibit PGCs at their original endodermal site, revealing a wide spatio-temporal window of PGC distribution. Our findings challenge the 'dogma' of active long-range PGC migration from the endoderm to the gonads. We therefore favor an alternative model based primarily on passive translocation of PGCs from the mesenchyme that surrounds the gut to the prospective gonad through the intercalar expansion of mesenchymal tissue which contains the PGCs. In summary, we (i) show differential pluripotency factor expression during primate embryo development and (ii) provide a schematic model for embryonic PGC translocation.

Key words: embryo / pluripotency factor / primordial germ cell / marmoset monkey

Introduction

The germ line comprises all cells that have the potential to pass (half of) their genetic material to an individual of the next generation. The mammalian germ line can be considered as a periodically reoccurring cycle of cells holding different states of inherent pluripotency (Leitch and Smith, 2013). The first clearly specified germ cells are the primordial germ cells (PGCs). Mouse PGCs are segregated from neighboring non-germ line cells by the expression of *Prdm1* (*Blimp1*) *Prdm14*, *Tfap2c* (*AP2gamma*), *fragilis* and *stella* (Saitou and Yamaji, 2010), and by around embryonic day (E)7.25 a founder population of ~40 PGCs has been established (Lawson and Hage, 1994). Human PGCs were originally identified based on their morphology which includes a large pale cytoplasm (Fuss, 1911; Felix, 1912; Politzer, 1933; Witschi, 1948) and later by histochemical characteristics such as alkaline phosphatase activity (Danziger and Kindwall, 1953). Since the invention of mouse transgenesis, mouse PGCs can be identified very impressively by germline-specific transgenic reporter constructs (e.g. Yeom *et al.*, 1996; Molyneaux *et al.*, 2001; Grabole *et al.*, 2013). However, in the absence of transgenic tools in primates, including humans, the detection and localization of PGCs in primates still depends either on cell morphology, which can be a rather ambiguous criterion with respect to the heterogeneous cell populations in an implantation embryo, or on validated and reliable endogenous germ line-specific markers. In general, it appears to be a characteristic of PGCs that they express pluripotency factors that are otherwise expressed

predominantly or even exclusively in the pluripotent cells of the preimplantation embryo and that are immediately down-regulated in all the somatic and extra-embryonic tissues of the implantation embryo (Zwaka and Thomson, 2005; Leitch and Smith, 2013). Embryonic stem (ES) cells are the prototype of pluripotent stem cells. Important key factors for the pluripotent state of cells include OCT4A (Nichols *et al.*, 1998; Niwa *et al.*, 2000; Boyer *et al.*, 2005), NANOG (Chambers *et al.*, 2007), SALL4 (Sal-like protein 4) (Elling *et al.*, 2006) and LIN28 (Yu *et al.*, 2007; West *et al.*, 2009). All four pluripotency factors have also been shown to play important roles for the establishment or maintenance of the mouse germ line (Kehler *et al.*, 2004; Chambers *et al.*, 2007; West *et al.*, 2009; Hobbs *et al.*, 2012). Altogether, these data strongly indicate a close interrelationship between pluripotent cells and the germ line.

In sharp contrast to the rapidly increasing knowledge of key events in mouse PGC development, only very little is known in humans. This is of special relevance since the tissues involved in PGC development in mice have no clear counterpart in the human. Probably most important, there is no apparent structure in the human equivalent to the mouse extra-embryonic ectoderm (De Felici, 2013), which plays a crucial role for PGC specification in the mouse via bone morphogenetic protein 4 signaling (Hayashi and Saitou, 2013). Studies of human PGCs during their specification and migration are still rare (De Felici, 2013). Many studies of human PGC development were performed 35–100 years ago (Fuss, 1911; Politzer, 1933; Witschi, 1948; McKay *et al.*, 1953; Fujimoto *et al.*, 1977) at a time when immunohistochemistry was not yet available. Therefore, protein expression data on different stages of human PGC development, especially the early stages, are still extremely fragmentary (Perrett *et al.*, 2008; Mollgard *et al.*, 2010; Mamsen *et al.*, 2012). Moreover, it will also be difficult to extend such studies in the future due to practical and ethical limitations.

Human PGCs can first be identified by the end of the third week post-conception (wpc) in the caudal wall of the yolk sac (Witschi, 1948; De Felici, 2013). At that time no gonads exist, instead the prospective gonads may be recognized only by a slight condensation of the celomic epithelium near the developing root of the gut mesentery. To develop a functional gonad, the PCGs must be translocated from their extra-embryonic site in the yolk sac endoderm to the intra-embryonic location of the forming gonads. Groundbreaking studies in the first half of the 20th century and also a few more recent studies suggest that PGCs actively migrate, in an ameboid way, over long distances across the embryo (Witschi, 1948). Their suggested trail is through the endodermal epithelium of the yolk sac and the yolk sac stalk (i.e. the epithelium of the vitellointestinal (omphaloenteric) duct) to the endoderm of the primitive gut, which is the dorsal continuation of the yolk sac endoderm. PGCs present in the endodermal gut epithelium were seen in human embryos from the fifth wpc onwards (Witschi, 1948; Mamsen *et al.*, 2012; De Felici, 2013). Thereafter, the PGCs leave the endodermal epithelium and invade the surrounding mesenchyme. Then they apparently move through the gut mesentery continuing their migration towards the gonadal ridge which harbors a sexually bipotential gonad at that stage. Active migration of PGCs appears to play an important role for the colonization of the mouse gonadal ridge (Molyneaux *et al.*, 2001; Richardson and Lehmann, 2010). It has been shown that the stromal cell-derived factor 1 (SDF-1)/SDF-1 receptor and the SCF (also known as kit-ligand, KL, or steel factor)/c-kit systems play roles during PGC migration in vertebrates (Pesce *et al.*, 1997; Molyneaux *et al.*, 2003; Farini *et al.*, 2007). Recently, Mollgard *et al.* (2010) and Mamsen *et al.* (2012) provided data suggesting that peripheral nerve fibers innervating the gut may serve as an anatomical guiding structure for PGCs. However, numerous aspects of PGC development and colonization of the primitive gonad by PGCs, especially in primates, are not understood.

In order to reduce the huge gap of knowledge regarding PGCs in primates we decided to investigate PGC development in the common marmoset monkey (*Callithrix jacchus*) embryo. The marmoset monkey is a small new world primate whose embryonic development was described in part decades ago (Phillips, 1976; Merker *et al.*, 1988). Interestingly, the marmoset's early post-implantation embryonic development is, for unknown reasons, significantly delayed compared with the human (Phillips, 1976; Li *et al.*, 2005). The marmoset monkey recently gained increasing attention due to its frequent use in biomedical studies, especially in reproduction, stem cell research and neurobiology. Moreover, the marmoset monkey was the first transgenic non-human primate with germ line transmission (Sasaki *et al.*, 2009). However, in sharp contrast to the relatively well-characterized post-natal testicular germ cell development (Chandolia *et al.*, 2006; Mitchell *et al.*, 2008; McKinnell *et al.*, 2009; Aeckerle *et al.*, 2012; Eildermann *et al.*, 2012; Lin *et al.*, 2012), embryonic germ cell development is poorly understood, or even uninvestigated, in the marmoset monkey (Li *et al.*, 2005).

Here, we studied PGC development in a set of 12 well preserved non-human primate embryos with a special focus on pluripotency factor protein expression by PGCs. By these means we also studied the *in situ* distribution of PGCs. We demonstrated a wide spatio-temporal window of PGC distribution and discovered an as yet unknown spatial proximity of PGCs in the endoderm to the site of the future gonad. This finding strongly questions the necessity of a long-range migration of PGCs. Based on this finding we favor the theory of a predominantly passive PGCs translocation from the endoderm to the gonad (Wrobel and Suss, 1998; Freeman, 2003) and provide a schematic model of passive PGC translocation.

Materials and Methods

Marmoset monkeys

All animal studies were performed according to the German Animal Protection Law. Animals were obtained from the self-sustaining marmoset monkey (*C. jacchus*) colony of the German Primate Center (Deutsches Primatenzentrum; DPZ) and housed according to the standard German Primate Center practice for common marmoset monkeys. Embryonic and fetal stages were obtained surgically by hysterotomy (licence number 42502-04-12/0708) or hysterectomy. Hysterectomy was used to obtain the E50 embryos since these embryos are too fragile to be retrieved by hysterotomy. All surgical work on the monkeys was performed by a veterinarian with several years of experience in handling and operating on marmoset monkeys. Samples taken before gestational Day 80 are referred to as embryos, older stages as fetuses (Chambers and Hearn, 1985).

Pregnancy timing, hysterotomy and embryo retrieval

Callithrix jacchus specimens used in this study were from the post-implantation period, between E50 and E75, previously found to be roughly equivalent to the embryonic period in human development between Carnegie stages 10 and 18 (O'Rahilly and Muller, 2001). Timed pregnancies ($n = 6$ yielding 12 embryos/fetuses) were obtained from animals in which

the stage of gestation was established from the post-ovulatory rise in progesterone (Harlow *et al.*, 1984), which was determined after blood collection from female marmoset monkeys twice weekly. For hysterotomy, which delivers embryos/fetuses in an optimal histological condition, animals were anesthetized with an i.m. injection of 0.5 ml/kg bodyweight *Göttinger Mischung II* (50 mg/ml ketamine (WDT, Garbsen, Germany), 10 mg/ml Xylazin (Bayer, Leverkusen, Germany), 10 mg/ml atropin (Eifelfango, Bad Neuenahr-Ahrweiler, Germany)) and 0.05 ml/animal diazepam (Ratiopharm, Ulm, Germany). The gravid uterus and the ovaries were delivered through a ventral midline incision in the abdominal wall under sterile conditions. The embryos or fetuses were removed through a horizontal incision in the uterine wall. The uterus and the abdominal wall were sutured surgically. To avoid postsurgical pain, 0.5 mg/animal i.m. meloxicam (Boehringer Ingelheim, Ingelheim am Rhein, Germany) was administered. In order to confirm the correct staging of the embryos before surgery, the development of the embryos/fetuses was observed via ultrasonography to ensure that they developed according to the expected growth curves. An overview of the embryos/fetuses used in this study is given in Table I. Embryos obtained before E90 were immediately fixed *in toto* in Bouin's solution to preserve tissue integrity. After that, fixed embryos were measured. E95 was cut into three pieces before fixation to prevent tissue disintegration. The crown-rump length, biparietal diameter and fronto-occipital diameter were measured using a caliper.

Table I Marmoset monkey (*Callithrix jacchus*) embryos/fetuses used in this study.

Embryo	CRL (mm)	BPD (mm)	FROD (mm)	E	Sex
1	ND	ND	ND	50	Female
2	ND	ND	ND	50	Female
3	ND	ND	ND	50	Male
4	9.1	2.5	3.9	65	Female
5	9.2	2.8	4.1	65	Male
6	10	2.9	4.4	68	Female
7	9.1	2.7	3.6	68	Male
8	10.5	3	4.7	72	Male
9	9.2	2.2	4.7	72	Female
10	ND	ND	ND	75	Female
11	ND	ND	ND	75	Male
12	ND	12.8	15.5	95	Male

CRL, crown-rump length; BPD, biparietal diameter; FROD, fronto-occipital diameter; E, embryonic day.

Tissue processing and immunohistochemistry

Retrieved embryos/fetuses were fixed overnight in Bouin's solution immediately after recovery resulting in excellent tissue preservation. After several washes in 70% EtOH for at least 2 days the embryos were embedded in paraffin and sectioned at 5 μm. During embedding the embryos were positioned to obtain either transverse or longitudinal sections. Tissue sections were deparaffinized, rehydrated and an antigen retrieval step was performed by microwaving the sections in citrate buffer (10 mM Tri-natriumcitratdihydrate in H_2O) for 10 min. Endogenous peroxidase was inhibited by incubation with peroxidase blocking reagent (DakoCytomation Carpinteria, CA, USA, LSAB+ system-HRP, K0679). Antibody specifications and dilutions are given in Table II. All incubation steps were in a humid chamber and incubations with the primary antibody were performed overnight at 4°C. DakoCytomation Universal LSAB Plus-kit including biotinylated second antibody polymer and horseradish peroxidase (HRP) conjugated streptavidin was employed for detection of bound primary antibody. 3,3′-diaminobenzidine (DAB) chromogen was used as substrate for the HRP and FastRed for alkaline phosphatase, and Mayer's hematoxylin was used as counterstain. Control stainings were carried out using IgG controls at the same protein concentration as the primary antibody instead of the specific primary antibody. Pictures were taken using a Zeiss microscope and the Nuance™ multispectral camera.

Marmoset monkey ES cell culture and ES cell samples for immunohistochemistry

Marmoset monkey ES cells (line cjes001) were published previously (Muller *et al.*, 2009). In order to obtain appropriate positive control samples for pluripotency factor immunohistochemistry, 10 cm dishes with undifferentiated marmoset ES cells cultured on mouse embryonic feeder cells for ~7 days were mechanically detached from the culture dish together with the feeder cell layer. Then the cells were transferred to a centrifuge tube and gently centrifuged at 200 g for 1 min. After centrifugation, the supernatant was replaced by Bouin's fixative, and the cells were fixed for one h. Subsequent tissue processing is described above. Finally, paraffin-embedded ES cells were sectioned at 5 μm.

Sex determination by PCR and immunohistochemistry

For sex determination of the embryos, genomic DNA was isolated from amnion, tip of the tail or a limb. Primers used for sex determination bind to

Table II Antibodies used in this study.

Antigen	Company	Order number	Host	Dilution
LIN28A	Cell Signaling Technology	#3978S	Rabbit (polyclonal)	1:100
NANOG	Cell Signaling Technology	#4903	Rabbit (monoclonal)	1:100
OCT4A (POU5F1)	Cell Signaling Technology	#2750	Rabbit (monoclonal)	1:200
SALL4	Abcam	#ab57577	Mouse (monoclonal)	1:200
VASA (DDX4)	R&D	#AF2030	Goat (polyclonal)	1:100
Goat IgG isotype control	Antibodies-online	ABIN376827	Goat	1:2500
Mouse IgG isotype control	Vector	I-1000	Mouse	1:1000
Rabbit IgG isotype control	Antibodies-online	ABIN376827	Rabbit	1:2500

conserved sites in the *DDX3* gene thus making them suitable for sex determination in mammals in general. *DDX3* is located on the X and the Y chromosome in variants of different lengths. Sequences of the primers are: forward 5′-GGWCGRACTCTAGAYCGGT-3′, reverse: 5′-GTRCAGATCTAYGAGGAAGC-3′. The expected sizes for PCR products are 176 bp for ddx3x (female) and 137 bp for ddx3y (male and female). Because of the cellular chimerism in twin marmosets, even in females a weak male-'specific' band can occur if the co-twin was a male, which is frequently the case. Therefore, samples from neonatal male and female animals (where sexing is possible based on the sex organs) were used as controls (Fig. 2G). In embryos at appropriate ages (≥E65) the sex of the embryo was also determined by the expression (or absence) of SOX9. SOX9 is a Sertoli cell-specific protein marking Sertoli cells from the onset of differentiation until adulthood. The sexes of all embryos used in this study are listed in Table I.

Results

Verification of the specificity and cross-reactivity of the antibodies used

The antibodies used in the present study were generated against epitopes of human OCT4A, NANOG, SALL4 and LIN28. In order to verify the cross-reactivity and to test the specificity of the antibodies for the respective marmoset monkey pluripotency factors, we applied the antibodies to Bouin-fixed and paraffin-embedded marmoset monkey ES cells grown on mouse embryonic fibroblasts (MEFs) as feeder cells. Figure 1A shows a hematoxylin-eosin-stained section. Marmoset monkey ES cells (red arrow) with a cuboidal shape can be clearly distinguished from mesenchymal mouse embryonic fibroblasts (blue

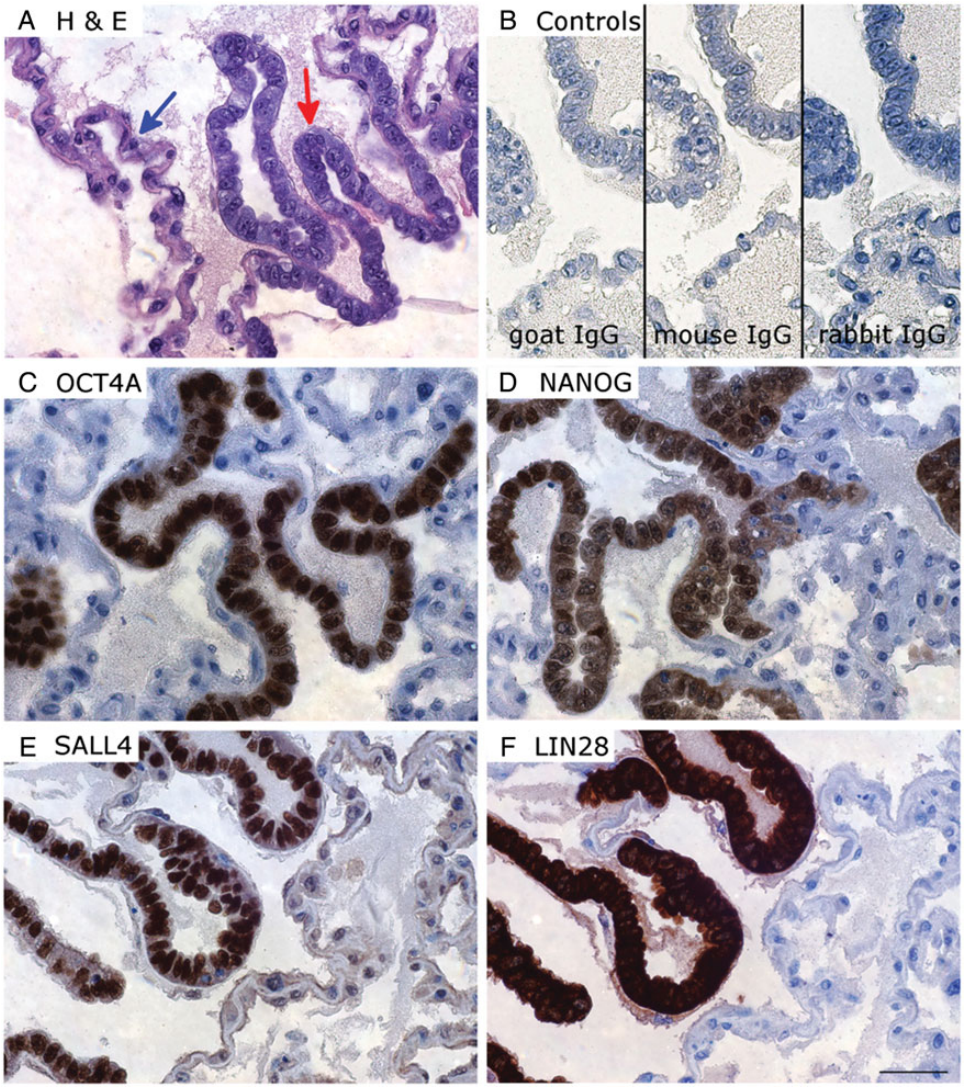

Figure 1 Validation of the antibodies for the marmoset monkey (*Callithrix jacchus*) pluripotency factors. (**A**) A section of paraffin-embedded embryonic stem (ES) cells stained with hematoxylin-eosin (H&E): Epitheloid ES cells with a cuboidal shape (red arrows) can be clearly distinguished from mesenchymal mouse embryonic fibroblasts (blue arrows), (**B**) IgG controls. (**C–F**) Staining with antibodies against OCT4A, NANOG, SALL4 (Sal-like protein 4) and LIN28, respectively. Scale bar represents 50 μm.

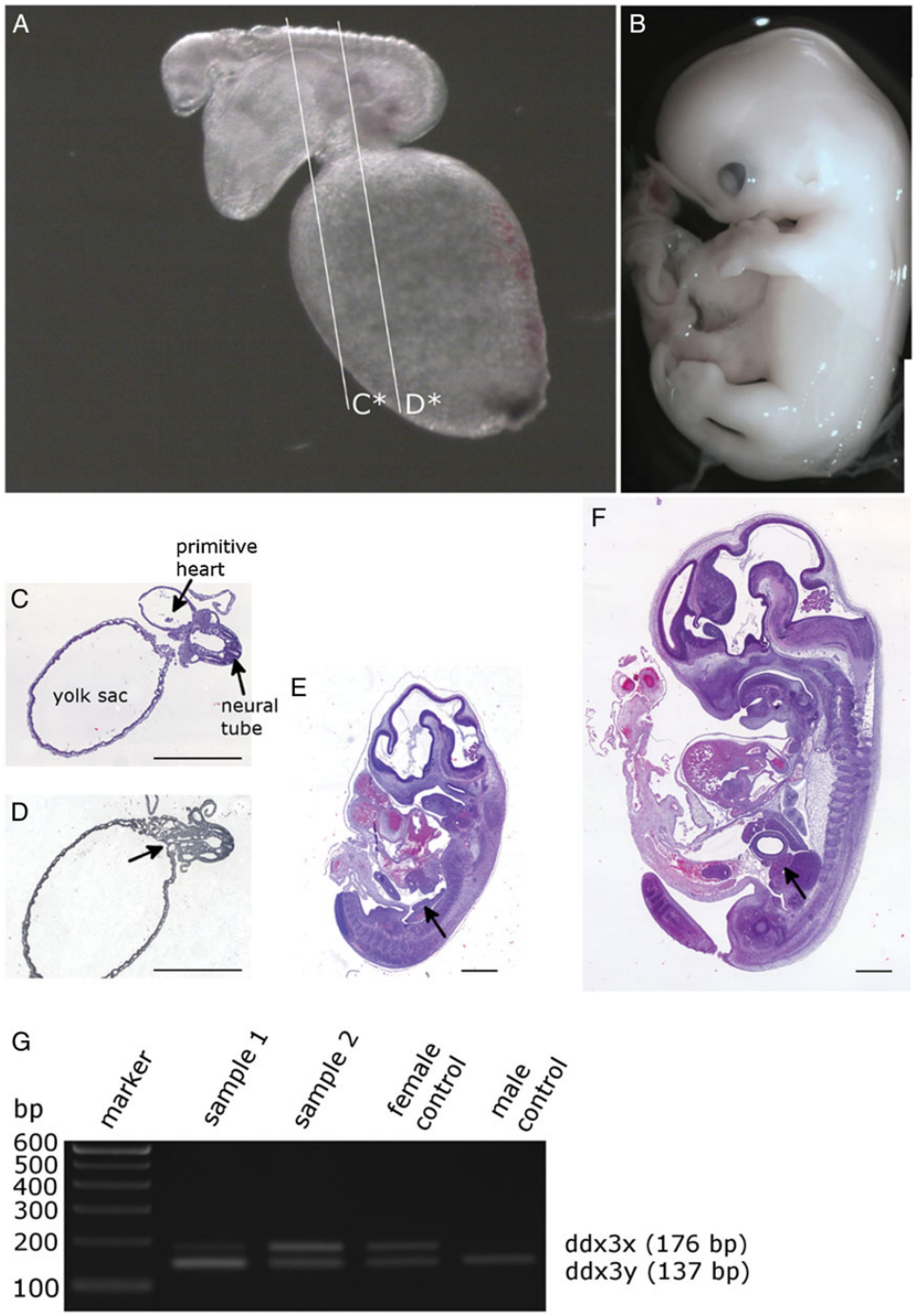

Figure 2 Characterization of marmoset monkey post-implantation embryonic development. The normal duration of pregnancy in marmosets is 143–145 days. (**A** and **B**) External morphology of marmoset embryos at embryonic day (E) 50 (Carnegie stage 10) and E75 (Carnegie stage 18), respectively. The crown-rump length of the embryo in (A) was 3.0 mm (picture was taken at 32-fold magnification). White lines in (A) indicate plane of the sections shown in (C) and (D). (B) (E75) was composed of two separate pictures. (**C** and **D**) Sections of a male marmoset embryo at E50 (same embryo as shown in (A)). Characteristic structures are indicated. (D) The duct connecting the yolk sac and embryo (arrow). (**E** and **F**) Sections of a male E65 and a male E75 ((F) the same embryo as (B)). The images reveal insights into development of the organ primordia. At E65, the indifferent gonad is clearly visible (arrow). Crown-rump length of the embryo is ~9 mm. At E75 crown-rump length of the embryo is ~12 mm. Scale bar represents 1 mm in (C)–(F). Sex of the embryos was determined by PCR on genomic DNA (**G**). Sample 1: male embryo, sample 2: female embryo. Skin biopsies from female and male neonatal marmosets were used as positive controls.

arrow). Figure 1B shows the negative controls (mouse/rabbit/goat IgG-control) exhibiting no staining signal. Figure 1C shows very intense nuclear OCT4A staining of marmoset ES cells, while the cytoplasm of ES cells is faintly stained and the MEFs are devoid of signal. Other somatic tissues (see below for embryos and data not shown) also exhibited no staining. Importantly, this antibody specifically binds to the N-terminal region of OCT4A and therefore specifically detects the pluripotency-associated form of OCT4, i.e. OCT4A. The NANOG antibody revealed clear nuclear but also some cytoplasmic staining of ES cells (Fig. 1D). No NANOG staining was observed in MEFs. SALL4 showed very intense nuclear staining of ES cells and only very faint signals in MEFs (Fig. 1E). In contrast, LIN28 exhibited strong cytoplasmic staining of ES cells and some nuclear signals (Fig. 1F). The LIN28 antibody also did not bind to MEFs. These data demonstrate the validity of the antibodies for the immunohistochemical detection of the marmoset monkey pluripotency markers OCT4A, NANOG, SALL4 and LIN28.

Developmental stages of marmoset monkey implantation embryos

The marmoset embryos studied were from the post-implantation period between E50 and E75 (Fig. 2). At E50, the embryo showed the first pharyngeal arch, otic vesicles, 17 somites flanking a neural tube open at both ends (Fig. 2A and C), a straight primitive heart tube contained in a large pericardial cavity and showing first rhythmic contractions, and a large yolk sac with an open connection to the primitive gut via the vitellinointestinal (omphaloenteric) duct (Fig. 2D, see also Fig. 3A). The region of the future gonad anlage was recognizable as a short stretch of high columnar celomic epithelium near the future root of the mesentery (Fig. 3, see below). A sexually indifferent gonad was found at E65, which is equivalent to Carnegie stage 16 (Fig. 2E, arrow), and at E68. At E72 and at E75 (equivalent to Carnegie stage 18) the gonad became sexually differentiated (female in the specimen shown) and separated from the underlying mesonephros by a short mesentery (Fig. 2F, arrow).

General overview of the expression of OCT4A, NANOG, SALL4 and LIN28

We investigated the presence of OCT4A, NANOG, SALL4 and LIN28 proteins at different stages of post-implantation embryo development (Figs 3–6). In general, OCT4A and NANOG were detectable exclusively in PGCs at all stages analyzed. The germ cell identity of the stained cells was confirmed by co-localization of the PGC markers with the germ cell marker VASA, which was detected in some marmoset embryos in migratory PGCs (Fig. 7 and data not shown for other developmental stages). In sharp contrast to OCT4A and NANOG, whose expression is restricted to PGCs in the E50 embryos, SALL4 and LIN28 were almost ubiquitously expressed at that stage. Interestingly, from E65 onwards, SALL4 and LIN28 were undetectable in the vast majority of somatic cells, while still strongly expressed in PGCs, indicating an abrupt switch-off of SALL4 and LIN28 in most somatic cells. Details are described in the following paragraphs.

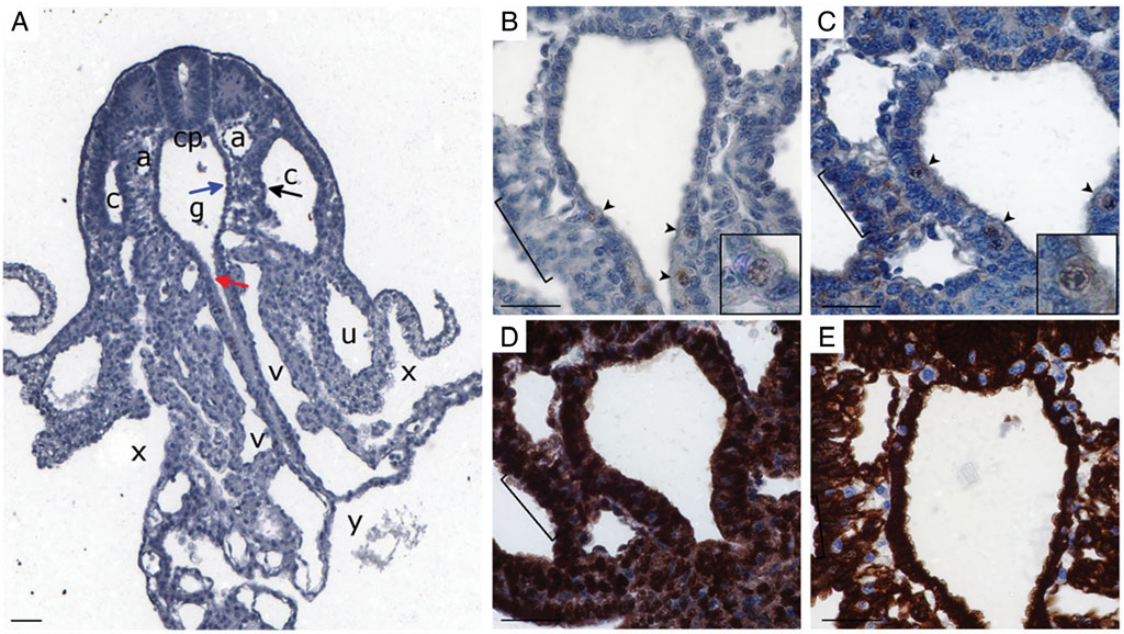

Figure 3 Pluripotency factor expression at E50. (**A**) The same embryo as Fig. 2C and D at a higher magnification. The red arrow highlights the endodermal epithelium lining the vitellinointestinal duct. The blue arrow highlights the endoderm of the primitive gut. The black arrow points at the site of the prospective gonadal ridge. (**B–E**) A higher magnification of the area shown in (A) containing germ cells in the lateral wall of the primitive gut. Sections were stained for OCT4A (B), NANOG (C), SALL4 (D) and LIN28 (E). Brackets mark the celomic epithelium of the prospective gonadal ridge. The OCT4A antibody specifically labeled nuclei of cells present in the endoderm at the junction between the yolk sac stalk and the primitive gut (arrowheads). The primordial germ cells (PGCs) were also stained by the NANOG antibody (C, arrowheads). In sharp contrast to OCT4A and NANOG, SALL4 (D) and LIN28 (E) showed rather ubiquitous expression, including the PGCs. a: dorsal aorta, c: celom, g: primitive gut, v: vitelline vessel, u: umbilical vein, x: exocoelom, cp: notochordal plate. Scale bars represent 50 μm.

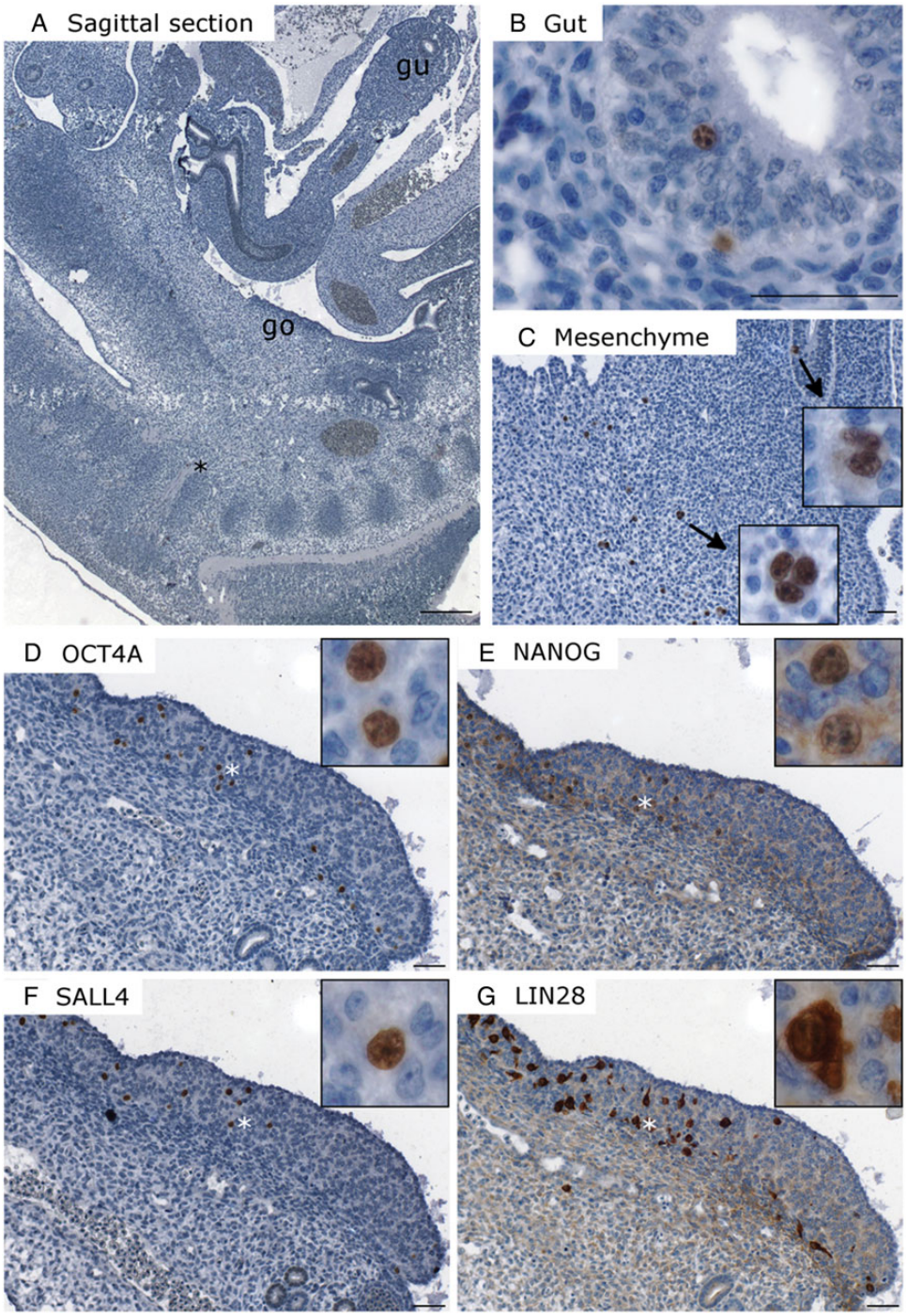

Figure 4 PGCs at E65. (**A**) A sagittal section. The gut is established as a closed tube (gu; see (B) for higher magnification) and the morphologically indifferent gonad is recognizable as a small but distinct thickening of the intermediate mesoderm (go; see (D)–(G) for higher magnification). OCT4A-positive PGCs were present in the endodermal gut epithelium, in the mesenchyme of the dorsal mesentery of the gut as well as in the retroperitoneal mesenchyme. The asterisk (middle, lower half Fig. 4A) highlights the position of an ectopic PGC associated with a peripheral nerve (see also Fig. 7B). (**B**) Higher magnification of (A) showing gut-epithelium-located PGCs. (**C**) Higher magnification of (A) showing gut-epithelium- and mesenchyme-located PGCs. (**D**–**G**) A fraction of the PGCs already reached the indifferent gonad (bipotential gonad). (D) OCT4A, (E) NANOG, (F) SALL4 and (G) LIN28. Scale bars represent 50 μm.

Pluripotency factor expression at E50

At gestational day E50, the embryo primarily consists of primitive derivatives of the three embryonic germ layers (Figs 2 and 3), and no chorda dorsalis had formed yet. Instead, the precursor cells of the chorda are still intercalated into the roof of the primitive gut forming the chordal plate. The only sign of presumptive gonad formation was a slight

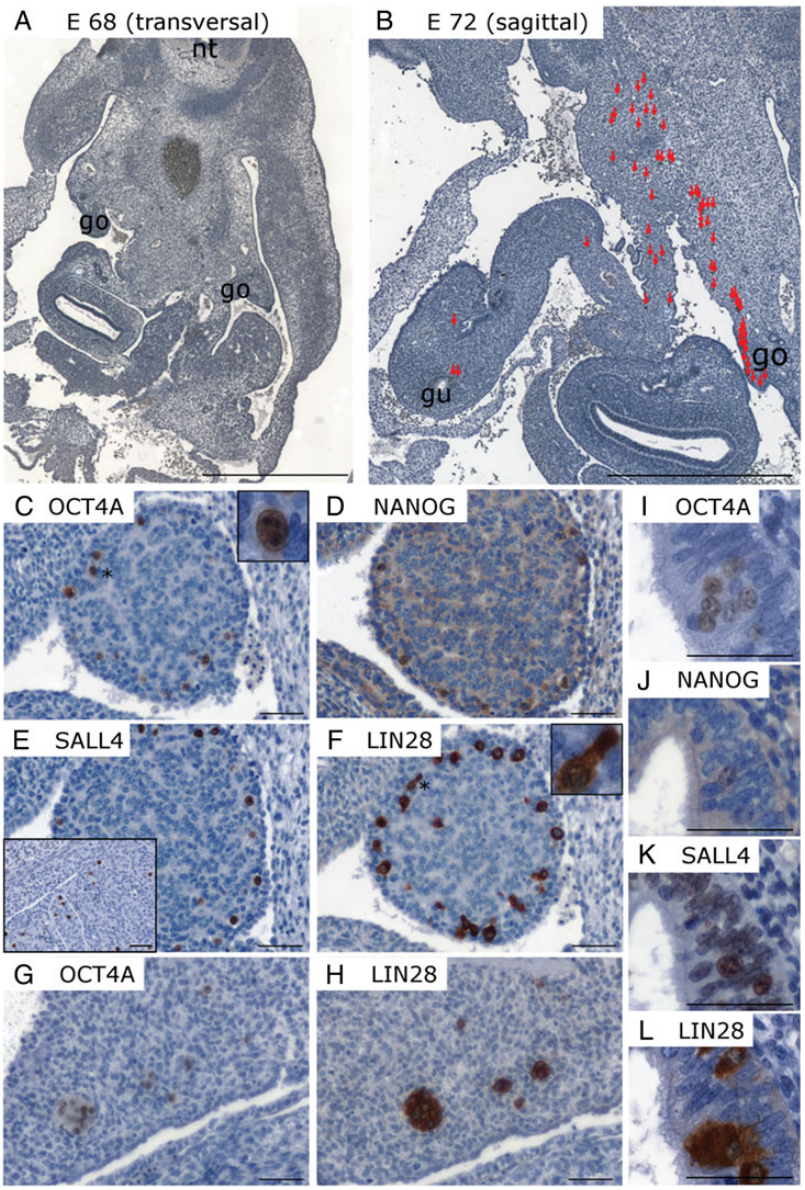

Figure 5 Aspects of the stages E68, E72 and E75. (**A**) A transverse section through an embryo at E68. The neural tube (nt) and the morphologically still undifferentiated gonads (go) are clearly visible. (**B**) A sagittal section at E72. Each single PGC (as identified by positive staining for OCT4A) is marked with a red arrow. (**C–F**) Transverse sections through a female gonad at E75. PGCs are located in the periphery of the gonad and express OCT4A (C), NANOG (D), SALL4 (E) and LIN28 (F). Inset in (E) shows an E75 male gonad. Formation of the prospective testicular cords was already initiated (indicated by the white dotted line). (**G** and **H**) Clusters of PGCs expressing OCT4A (G) and LIN28 (H) present in the retroperitoneal compartment of the female E75. (**I–L**) PGCs present in the gut epithelium at E75. They express OCT4A (I), NANOG (J), SALL4 (K) and LIN28 (L) and show no signs of apoptosis. gu: gut epithelium, go: gonad. Scale bar represents 1 mm (A and B) and 50 μm (C–L).

thickening of the celomic epithelium lateral to the vitellinointestinal duct but ventral to the paired aorta (Fig. 3A). PGCs, not easily recognized by their 'typical' morphology in the routinely stained sections (Fig. 3B), were specifically labeled by the OCT4A antibody. PGCs had a large, roundish nucleus, and the cells were present in the caudal endoderm lining the yolk sac stalk and the primitive gut (Fig. 3B). PGCs exhibiting rather round nuclei could be distinguished from the majority of the surrounding somatic cells, which also have large, but rather oval or polygonal nuclei. However, OCT4A-positive cells mostly lacked the large pale cytoplasm. No other cell type was found to be labeled by the OCT4A antibody. Similarly, the NANOG antibody produced a nuclear staining and, like in the ES cells (Fig. 1), some cytoplasmic staining (Fig. 3C). Both OCT4A and NANOG staining were weaker than in ES cells and in later PGC stages. In sharp contrast to OCT4A and NANOG, SALL4 and LIN28 did not exhibit a PGC-specific expression but a positive reaction in the vast majority of all cells at the E50 stage (Fig. 3D and E). Only few somatic cells were negative for SALL4 and LIN28.

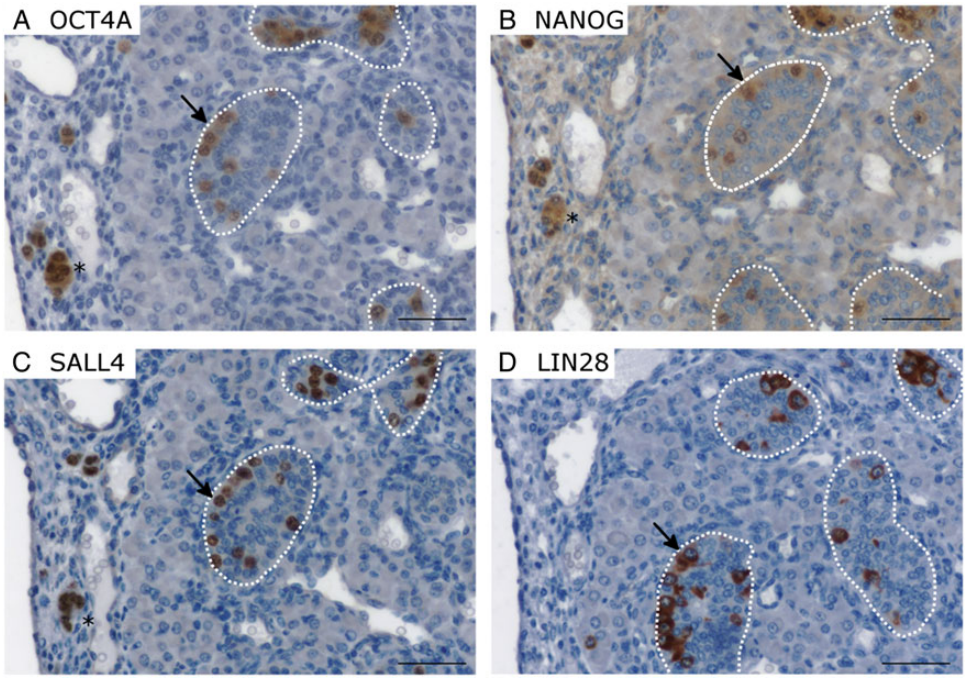

Figure 6 The E95 gonad is a fetal testis. At E95 the vast majority of germ cells which reached the gonad are enclosed in testicular cords (indicated by arrows); only few germ cell clusters were still located at the junction between the testis and the prospective epididymis, i.e. the forming *rete testis* (indicated by *). Intratubular germ cells still express high levels of OCT4A (**A**), NANOG (**B**), SALL4 (**C**) and LIN28 (**D**). However, there were also germ cells expressing little or even no OCT4A and NANOG (not shown). No germ cells were detected outside the gonads. Scale bar represents 50 μm.

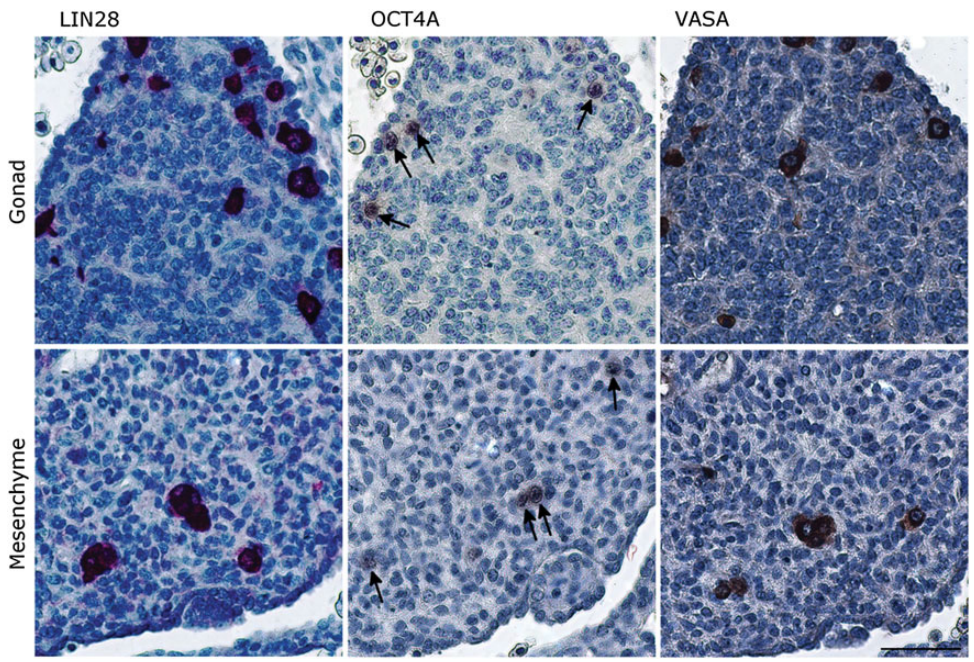

Figure 7 VASA is detectable in cells expressing LIN28 and OCT4A. At E75 the germ cell marker VASA was detectable in cells expressing LIN28 and OCT4A (indicated by arrows) in the female gonad (upper panel) and the mesenchyme (lower panel). Scale bar represents 50 μm.

With regard to the topographical proximity to the site of the prospective gonad, specifically labeled PGCs in E50 embryos were detected in the endoderm of the yolk sac stalk (red arrow in Fig. 3A) and of the primitive gut (blue arrow in Fig. 3A), and some of these PGCs were present in basal compartment of the epithelium—i.e. close to the basement membrane—of the gut tube (Fig. 3A–C). In this position they are very close (*c.* 50 μm) to the site where the gonadal ridge started to form (Fig. 3B–D, brackets).

PGCs at E65

At E65 the gut had developed into a closed tube with a proper mesentery. The morphologically indifferent gonad was recognizable as a small but distinct thickening of the intermediate mesoderm bulging from the posterior body wall (Fig. 4A, see also Fig. 2 for the overview). The gonad was covered by a single-layered epithelium, the prospective peritoneum. There is no histological evidence of epithelial organization within the gonadal primordium, and the male and female gonads are morphologically indistinguishable even though SOX9, a male (pre-) Sertoli cell-specific protein, was detectable in the male gonadal primordium, while this antigen was undetectable in the female (data not shown). OCT4A-positive PGCs were still detected in the endodermal gut epithelium (Fig. 4B) but no PGCs were detected in the densely packed mesenchyme underlying the gut epithelium. Some PGCs were localized in the root of the mesentery (Fig. 4C) as well as in the retroperitoneal mesenchyme. A substantial fraction of the PGCs had already reached the indifferent gonad (Fig. 4D–G) occupying mostly the proximal part of the gonad, while the distal part contained only few scattered PGCs. PGCs staining positive for OCT4A, NANOG, SALL4 and LIN28 were found in the gonads but also at many extra-gonadal sites (data not shown for E65, but see Figs 5, 7 and 8).

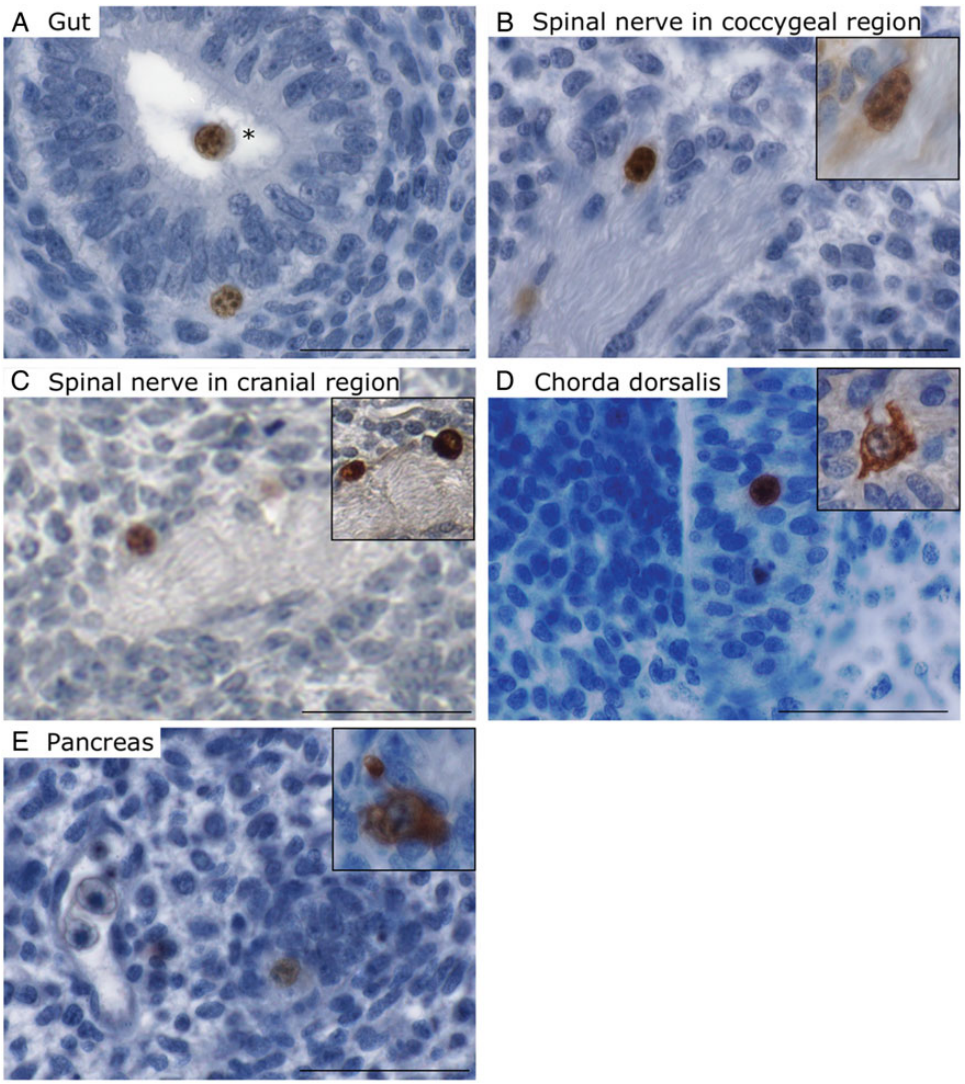

Figure 8 PGCs at atypical/ectopic sites detected in different embryos at different developmental stages. At E65 one OCT4A-positive PGC was detected in the lumen of the gut with no evident contact to the epithelium (**A**). Another PGC was present in a forming spinal nerve in the coccygeal region and was clearly positive for OCT4A (**B**) and NANOG (inset in B). In an E68 embryo we localized an OCT4A and LIN28-positive PGC in a peripheral nerve in the cranial region of the embryo (**C**). Another PGC (OCT4A and LIN28-positive) found in the female E72 was present in the Chorda dorsalis (**D**). An E75 stage also presented one PGC in the pancreas (**E**). Scale bar represents 50 μm.

PGCs at E68, E72 and E75

At E68 the gonads were morphologically undifferentiated. Specifically labeled PGCs were detected, as at E65, in the developing gut including the mesentery, in retroperitoneal tissue and in the gonads (Fig. 5A). At E72, PGCs were still seen in the gut epithelium as well as in the dense mesenchyme surrounding the gut epithelium (Fig. 5B), in the root of the mesentery and in the retroperitoneal mesenchyme. PGCs expressed all four markers at all sites during all stages (Fig. 5C–L for E75; data not shown for E68 and E72). The female gonad at E75 contained PGCs positive for OCT4A, NANOG, SALL4 (all nuclear) and LIN28 (mostly cytoplasmic). OCT4A signals appeared most intense in the nucleoli of the PGCs (inset in Fig. 5C). In the E75 male gonad (inset in Fig. 5E), which exhibits formation of the prospective testicular cords (indicated by the white dotted line), PGCs were present inside and outside the forming cords. Numerous PGCs were still detectable outside the gonads in the mesenchyme (Fig. 5G and H) and even in the gut epithelium (Fig. 5I–L). Besides single PGCs, several clusters of PGCs were seen in the mesenchyme (Fig. 5G and H). The wide distribution of PGCs at the E72 stage is illustrated in Fig. 5B. Because of the low-power magnification of this overview, individual PGCs are not easily visualized; therefore individual PGCs are identified by a red arrow (Fig. 5B). No sex-specific differences in PGC distribution were found until the onset of histological differentiation of the gonads (see below).

The male E95 gonad is a fetal testis

In male E95 the germ cells are generally enclosed in testicular cords; only a few germ cell clusters were still located in the developing rete testis (Fig. 6). Intratubular germ cells, called gonocytes (if not in contact with the basal lamina of the cord) or pre-spermatogonia (if already in contact with the basal lamina), still express OCT4A, NANOG, SALL4 and LIN28 (Fig. 6A–D). OCT4A as well as NANOG showed faint cytoplasmic signals in addition to robust nuclear signals, while SALL4 was strictly nuclear. LIN28 was almost exclusively cytoplasmic. No germ cells were detected outside the gonads or the rete testis at this stage.

PGCs at atypical/ectopic sites

While the vast majority of PGCs detected were present in one of the tissues between the yolk sac epithelium and the gonads, we also localized some PGCs at atypical (i.e. ectopic) sites. At E65 we found one OCT4A-positive PGC in the lumen of the gut with no contact to the epithelium (Fig. 8A). Another PGC was present in a developing peripheral nerve in the coccygeal region far 'beyond' the gonad as physiologically final destination (Fig. 8B). In an E68 embryo we localized one PGC in a peripheral nerve in the cranial region of the embryo (Fig. 8C). Another PGC was found in a female at E72 in the Chorda dorsalis (Fig. 8D). An E75 embryo presented a PGC in the pancreas (Fig. 8E).

Discussion

This first systematic investigation of PGC development in a non-human primate provides detailed embryological and morphological data and combines them to provide novel insights into the spatio-temporal expression of a quartet of pluripotency factors during primate embryogenesis.

The timing of PGC development described in the present report is probably appreciated best in comparison with human gestation, which is on average 267 days while marmoset monkey gestation is 143–145 days (i.e. only ~54% of the human). However, in the marmoset embryo the Carnegie stage 10 is reached at E50 while human embryos reach this stage at around E23. Carnegie stage 10 is the stage where PGCs can first be identified in the human embryo yolk sac (De Felici, 2013). Similarly, the marmoset monkey embryo at E75 represents Carnegie stage 18, while this stage is reached in the human at around E44. These data are supported by findings reported previously (Phillips, 1976; Merker *et al.*, 1988; Li *et al.*, 2005) and indicate that the period of PGC specification and migration is significantly delayed in marmoset monkeys compared with the human despite the significantly shorter overall gestational period of the marmoset monkey. It remains to be determined when this delay is 'ironed out' during further development.

In the absence of appropriate markers, PGCs were described in most publications as histologically easily identifiable cells because of their large spherical or oval shape and their clear cytoplasm in bright field microscopy (Politzer, 1933; Witschi, 1948; Fujimoto *et al.*, 1977). They are also reported to have a large nucleus, usually with one or two prominent nucleoli (Pereda *et al.*, 2006). However, these widely accepted morphological characteristics of PGCs may apply only to later PGC stages in humans. Indeed, already Witschi emphasized that yolk sac-located human PGCs 'differ little from associated somatic cells, and it is difficult to identify them with certainty' (Witschi, 1948). Our study confirmed that early PGCs are morphologically rather similar to the neighboring somatic cells and only the OCT4A and NANOG staining allowed us to identify them with some certainty. Interestingly, even the PGCs in the marmoset embryos located in the mesenchyme of the mesentery or the retroperitoneal space are not always in agreement with the description of respective human PGCs. While some PGCs exhibited the expected morphology, other clearly stained cells were rather small and had apparently oval nuclei making them morphologically difficult to distinguish from the neighboring somatic cells. Differences in the morphology of human PGCs during different phases of development and migration have been also described by Fujimoto *et al.* (1977). That pluripotency factor-positive cells in this study, even those with unexpected morphology, are indeed germ cells has been confirmed by VASA staining of the respective cells in consecutive sections (Fig. 7). VASA was detectable in many extra-gonadal PGCs as well as in all morphologically recognizable gonadal germ cells of both sexes. This is in contrast to findings in the developing human gonad, where VASA-negative germ cells were also identified (Anderson *et al.*, 2007; Gkountela *et al.*, 2013). These differences may be due to biological or technical reasons: it is possible that the different expression patterns simply reflect species-specific differences. Furthermore, the developmental stages analyzed in the respective studies may not be directly comparable due to the developmental delay of the marmoset monkey. Finally, in one study (Anderson *et al.*, 2007) a different VASA antibody was used than in the present and a previous study (Gkountela *et al.*, 2013). Despite the VASA localization in embryonic marmoset germ cells, we cannot exclude that some of the pluripotency marker-positive cells may belong to an alternative stem or progenitor cell population unrelated to germ cells. Nevertheless, it has been shown that tissue-specific *Oct4* deletion does not affect the maintenance of the adult stem cell population or homeostasis of different mouse tissues including the intestinal epithelium, bone marrow (hematopoietic and mesenchymal lineages), hair follicle, brain and liver (Lengner *et al.*, 2007). This finding rather supports the view that OCT4-positive cells found in our study do not contribute to other cell populations. Interestingly, the *OCT4* gene is alternatively spliced (Wang and Dai, 2010), i.e.

there is an *OCT4A* and an *OCT4B* transcript and only *OCT4A* is specifically associated with pluripotency. The OCT4A antibody used in the present study, produced specific, robust and reproducible results in immunohistochemistry and therefore, together with the recent reports by Gkountela *et al.* (2013) and McKinnell *et al.* (2013), represents significant progress regarding the analysis of OCT4 protein expression in the primate germ line. This is important since in a previous study we found several OCT4 antibodies to be non-specific (Warthemann *et al.*, 2012).

Some data on OCT4 and NANOG in human and marmoset premeiotic germ cells are already available (Rajpert-De Meyts *et al.*, 2004; Anderson *et al.*, 2007; Kerr *et al.*, 2008; Perrett *et al.*, 2008; Gkountela *et al.*, 2013; McKinnell *et al.*, 2013). However, the information on LIN28 in primate PGCs is still scarce (Gillis *et al.*, 2011; Aeckerle *et al.*, 2012; Childs *et al.*, 2012) and that on SALL4 in PGCs is, to our knowledge, even more preliminary (Eildermann *et al.*, 2012). Furthermore, the data on the latter factors mainly refer to late PGCs. In contrast, we show here that both SALL4 and LIN28 are already expressed during the very early phases of PGC development.

Considering that SALL4 as well as LIN28 are strongly expressed not only by pluripotent stem cells and PGCs, but also by some somatic (multipotent) progenitor cells, the finding of almost ubiquitous expression may rather reflect an undifferentiated progenitor stage than a pluripotent state of the E50 somatic cells. In contrast to SALL4 and LIN28, OCT4A and also NANOG are strictly associated with pluripotency.

Upon arrival in the gonad, male PGCs are enclosed by Sertoli cells during formation of the fetal testicular cords. During this process, the PGCs start down-regulating the expression of OCT4A and NANOG in most germ cells (which are now called gonocytes), and at birth these two key pluripotency factors are only detectable in a fraction of marmoset germ cells (data not shown for older stages, see also (McKinnell *et al.*, 2013)). In adult primate testes (including human, baboon, rhesus macaque and marmoset monkey) we were unable to detect either OCT4A or NANOG (data not shown). In contrast to these factors, LIN28 and SALL4 are also expressed post-natally at significant levels: while SALL4 can be robustly detected in all diploid male germ cells up to the A_{pale} spermatogonial stage (Eildermann *et al.*, 2012), LIN28 is seen in gonocytes and a very small subpopulation of spermatogonia in adult testis (Aeckerle *et al.*, 2012). Hence, SALL4 and LIN28 can serve as germ cell markers from the migratory stage of PGCs up to the postnatal phase. The early down-regulation and subsequent lack of expression of OCT4A and NANOG during testis development suggests that the Sertoli cells may play a crucial role in the transition from the pluripotent state of the PGCs (Shamblott *et al.*, 1998) to the unipotent state of the gonocytes. However, the specific signals provided by the somatic environment which influence germ cell potential remain to be identified. Unfortunately no female specimen of E95 was available for this study. Interestingly, the histological male-specific embryonic rearrangements of the gonads were not associated with a detectable change in the expression of OCT4A, NANOG, SALL4 or LIN28, either compared with earlier male stages or with PGCs in the corresponding female gonads.

In general it was unexpected that in the E65–E75 stages PGCs were seen at all sites analyzed (gut epithelium, root of the mesentery, mesenchyme of the retroperitoneum, gonad primordium), and no clear shift of a major PGC population from the gut endoderm to the gonad was evident during PGC colonization of the gonad. We found PGCs at their final destination in the gonadal primordium by E65. On the contrary, we still found PGCs in the E75 and even the ~E90 gut endoderm, when gonadal as well as gut differentiation was already at an advanced stage, i.e. the embryo had already undergone the transition to a fetus. The gut PGCs located in the endoderm did not exhibit histological signs of apoptosis, although this route of PGC depletion was suggested for the human (Mamsen *et al.*, 2012) and the mouse embryo (Pesce *et al.*, 1993; Stallock *et al.*, 2003). Future analyses will address this issue also in marmoset monkey embryos. We found no PGCs in the celomic epithelium as reported by McKay *et al.* (1953) for a 5 mm human embryo or by Fujimoto (1977) for a human 5-week post-conception (wpc) embryo. This appears to be a difference between marmoset and human embryos. A relatively wide spatio-temporal distribution pattern of PGCs was also reported for human embryos ranging from the 4th wpc to the 14th wpc (Fujimoto *et al.*, 1977; Mamsen *et al.*, 2012). This appears to be a physiologically remarkable situation: Why are there so many PGCs still in the gut epithelium, while the gonad has already initiated differentiation? Do these gut PGCs still have the chance to enter the gonad and contribute to adult gametogenesis? If not, why did they fail to reach the gonads at the appropriate time? Indeed, as recently discussed (Byskov *et al.*, 2011), the latest time point at which PGCs may enter the developing gonad is still not clear.

In contrast to the predominant opinion of a coordinated long-range migration of the PGC population from the endoderm to the gonad (Witschi, 1948; Fujimoto *et al.*, 1977), we suggest that PGCs are allocated to different tissues (endodermal epithelium versus mesodermal mesenchyme) via active short-range migration during early embryonic development (in the marmoset between E50 and E65) and that they are then further distributed and translocated, predominantly passively, by the growth, proliferation and rearrangement of the respective tissue harboring the PGCs in the embryo. Indeed, in E50 embryos, the distance between endodermal PGCs and the site of the prospective gonad is only ~50 μm. Figure 9 provides a simple model for this hypothesis. This model is also in agreement with careful morphological observations in bovine embryos made by Wrobel and Suss (1998), who concluded that the assumptions of a long-range chemo-attraction of the PGCs by the gonadal ridge, including active migration of PGCs, is not necessary to explain the initial settlement of bovine PGCs in the gonadal ridge. This view was further elaborated by Freeman (2003). However, future studies need to clarify whether the proliferation and apoptosis indices of PGCs and the somatic tissues at different sites in the embryo correspond to our model. Nevertheless, PGC migration appears to be essential over short distances during the early embryonic phase, particularly for reaching the lateral position of the primitive gut as well as for crossing the basal lamina of the endodermal epithelium and subsequent entry into the surrounding mesenchyme. The finding of PGCs in the Chorda dorsalis could be explained by PGC movements into a dorsal position of the primitive gut at the phase when the Chorda dorsalis is transiently intercalated into the roof of the gut (Fig. 3A). During re-separation of the Chorda from the dorsal gut, PGCs may be co-translocated from the roof of the primitive gut to the Chorda dorsalis.

Finally, besides ectopic PGCs we also observed strong clustering of PGCs in some embryos at different sites, predominantly in the root of the mesentery and in the retroperitoneal tissue. At present it remains unclear whether this is a marmoset monkey-specific phenomenon or whether the absence of such PGC clusters is a human-specific characteristic.

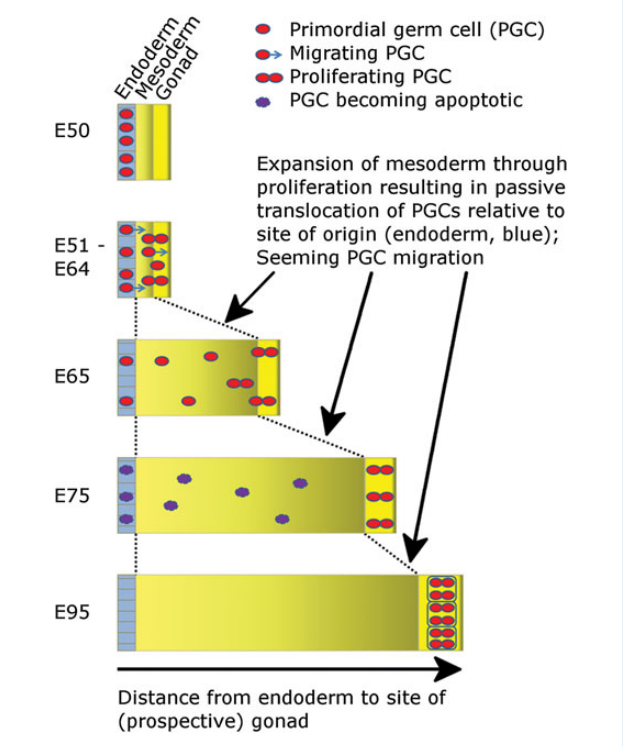

Figure 9 Model of PGC translocation from the endoderm to the gonad in the marmoset monkey. The model is based on the one hand on PGC proliferation, survival, and apoptosis and on the other hand on growth of somatic tissues surrounding the PGCs, rather than active PGC migration. At E50 the PGCs are exclusively present in the endoderm. Between E50 and E65 some PGCs actively leave the endodermal epithelium crossing the basal lamina thereby entering the surrounding mesenchyme. Importantly, at this early stage the site of the prospective gonad is very close to the endoderm. At E65, PGCs can be seen at all sites constituting the 'migration' route of the PGCs: in the endoderm, the mesenchyme and the gonads. The distance between the endoderm and the gonads constantly increases by intercalary proliferation and growth of the mesenchymal structures linking the endoderm and the gonad. Therefore those PGCs located close to the site of the prospective gonad at earlier stages are passively translocated from the endoderm towards the gonad. Those PGCs close to or within the gonad proliferate and survive. In contrast to these gonadal PGCs, the model further hypothesizes that PGCs distant from the gonad at > E75 stages are depleted by apoptosis. At E95, only gonadal germ cells are left.

Summary and Conclusion

We provide the first detailed analysis of the expression of four key pluripotency factors during primate post-implantation embryo development. We show that OCT4A and NANOG proteins are present early in development and are specifically restricted to PGCs, while SALL4 and LIN28 are only useful for the detection of PGCs at later stages, since these factors can also be detected in most somatic cells of E50 embryos. We further show that PGCs in the marmoset monkey can form clusters. There is a wide spatio-temporal window of 'PGC migration' since PGCs can be found very early in the gonadal primordia and, at later stages, are still in the gut endoderm. Most interestingly, the distance between endodermal PGCs and the site of the prospective gonad in E50 embryos is very short. We interpret these findings as supporting the view that active long-range PGC migration is not necessary in the mammalian embryo. As an alternative we suggest that a predominantly intercalating mesenchymal tissue expansion may contribute to the relative translocation of PGCs from their origin in the endodermal epithelium to the gonadal primordium. However, further investigations are needed to better understand these morphogenetic processes as well as the molecular and cellular changes of the PGCs during these phases of development in primate embryos.

Acknowledgement

We thank Nicole Umland, Marion Seidel, Angelina Berenson and Simone Luert for excellent technical assistance and Dr Christian Roos from the Primate Genetics Laboratory at the German Primate Center for the primer sequences for sex determination. We appreciate the assistance of Ellen Wiese. Nelia Aeckerle was a PhD student of Biology at the Jacobs University Bremen. We gratefully acknowledge the support of Prof. Alexander Lerchl and Prof. Matthias Ullrich (Jacobs University Bremen).

Authors' roles

N.A.: study design, collection and assembly of data, data analysis and interpretation, manuscript writing, final approval of manuscript. C.D.: provision of study material, final approval of manuscript. K.D.: provision of study material, final approval of manuscript. C.V.: data analysis and interpretation, manuscript writing, final approval of manuscript. R.B.: study design, financial support, data analysis and interpretation, manuscript writing, final approval of manuscript.

Funding

This study was supported in part by BMBF Federal Ministry of Education and Research grant 01GN0810 entitled 'Pluripotent cells in primate testes' to R.B. and by the German Research Foundation by an unrestricted grant within the Research Unit 'Germ Cell Potential (FOR – BE 2296/6-2)' to R.B. Funding to pay the open access publication charges for this article was provided by the German Primate Center.

Conflict of interest

The authors declare that there is no conflict of interest that could be perceived as prejudicing the impartiality of the research reported.

References

Aeckerle N, Eildermann K, Drummer C, Ehmcke J, Schweyer S, Lerchl A, Bergmann M, Kliesch S, Gromoll J, Schlatt S *et al.* The pluripotency factor LIN28 in monkey and human testes: a marker for spermatogonial stem cells? *Mol Hum Reprod* 2012;**18**:477–488.

Anderson RA, Fulton N, Cowan G, Coutts S, Saunders PT. Conserved and divergent patterns of expression of DAZL, VASA and OCT4 in the germ cells of the human fetal ovary and testis. *BMC Dev Biol* 2007;**7**:136.

Boyer LA, Lee TI, Cole MF, Johnstone SE, Levine SS, Zucker JP, Guenther MG, Kumar RM, Murray HL, Jenner RG *et al.* Core

transcriptional regulatory circuitry in human embryonic stem cells. *Cell* 2005;**122**:947–956.

Byskov AG, Hoyer PE, Yding Andersen C, Kristensen SG, Jespersen A, Mollgard K. No evidence for the presence of oogonia in the human ovary after their final clearance during the first two years of life. *Hum Reprod* 2011;**26**:2129–2139.

Chambers PL, Hearn JP. Embryonic, foetal and placental development in the common marmoset monkey (*Callithrix jacchus*). *J Zool* 1985;**207**: 545–561.

Chambers I, Silva J, Colby D, Nichols J, Nijmeijer B, Robertson M, Vrana J, Jones K, Grotewold L, Smith A. Nanog safeguards pluripotency and mediates germline development. *Nature* 2007;**450**:1230–1234.

Chandolia RK, Luetjens CM, Wistuba J, Yeung CH, Nieschlag E, Simoni M. Changes in endocrine profile and reproductive organs during puberty in the male marmoset monkey (*Callithrix jacchus*). *Reproduction* 2006; **132**:355–363.

Childs AJ, Kinnell HL, He J, Anderson RA. LIN28 is selectively expressed by primordial and pre-meiotic germ cells in the human fetal ovary. *Stem Cells Dev* 2012;**21**:2343–2349.

Danziger L, Kindwall JA. Thyroid therapy in some mental disorders. *Dis Nerv Syst* 1953;**14**:3–13.

De Felici M. Origin, migration, and proliferation of human primordial germ cells. In: Coticchio G, Albertini DF, De Santis L (eds). *Oogenesis*. London: Springer, 2013, 364.

Eildermann K, Aeckerle N, Debowski K, Godmann M, Christiansen H, Heistermann M, Schweyer S, Bergmann M, Kliesch S, Gromoll J *et al.* Developmental expression of the pluripotency factor sal-like protein 4 in the monkey, human and mouse testis: restriction to premeiotic germ cells. *Cells Tissues Organs* 2012;**196**:206–220.

Elling U, Klasen C, Eisenberger T, Anlag K, Treier M. Murine inner cell mass-derived lineages depend on Sall4 function. *Proc Natl Acad Sci USA* 2006;**103**:16319–16324.

Farini D, La Sala G, Tedesco M, De Felici M. Chemoattractant action and molecular signaling pathways of Kit ligand on mouse primordial germ cells. *Dev Biol* 2007;**306**:572–583.

Felix W. The development of the urinogenital organs. In: Keibel F, Mall FP (eds). *Manual of Human Embryology II*. J. B. Lippincott Company, The Washington Square Press, Philadelphia, USA, 1912.

Freeman B. The active migration of germ cells in the embryos of mice and men is a myth. *Reproduction* 2003;**125**:635–643.

Fujimoto T, Miyayama Y, Fuyuta M. The origin, migration and fine morphology of human primordial germ cells. *Anat Rec* 1977;**188**:315–330.

Fuss A. Über extraregionare Geschlechtszellen bei einem menschlichen Embryo von 4 Wochen. *Anat Am* 1911;**39**:407–409.

Gillis AJ, Stoop H, Biermann K, van Gurp RJ, Swartzman E, Cribbes S, Ferlinz A, Shannon M, Oosterhuis JW, Looijenga LH. Expression and interdependencies of pluripotency factors LIN28, OCT3/4, NANOG and SOX2 in human testicular germ cells and tumours of the testis. *Int J Androl* 2011;**34**:e160–e174.

Gkountela S, Li Z, Vincent JJ, Zhang KX, Chen A, Pellegrini M, Clark AT. The ontogeny of cKIT+ human primordial germ cells proves to be a resource for human germ line reprogramming, imprint erasure and *in vitro* differentiation. *Nat Cell Biol* 2013;**15**:113–122.

Grabole N, Tischler J, Hackett JA, Kim S, Tang F, Leitch HG, Magnusdottir E, Surani MA. Prdm14 promotes germline fate and naive pluripotency by repressing FGF signalling and DNA methylation. *EMBO Rep* 2013; **14**:629–637.

Harlow CR, Hearn JP, Hodges JK. Ovulation in the marmoset monkey: endocrinology, prediction and detection. *J Endocrinol* 1984;**103**:17–24.

Hayashi K, Saitou M. Stepwise differentiation from naive state pluripotent stem cells to functional primordial germ cells through an epiblast-like state. *Methods Mol Biol* 2013;**1074**:175–183.

Hobbs RM, Fagoonee S, Papa A, Webster K, Altruda F, Nishinakamura R, Chai L, Pandolfi PP. Functional antagonism between Sall4 and Plzf defines germline progenitors. *Cell Stem Cell* 2012;**10**:284–298.

Kehler J, Tolkunova E, Koschorz B, Pesce M, Gentile L, Boiani M, Lomeli H, Nagy A, McLaughlin KJ, Scholer HR *et al.* Oct4 is required for primordial germ cell survival. *EMBO Rep* 2004;**5**:1078–1083.

Kerr CL, Hill CM, Blumenthal PD, Gearhart JD. Expression of pluripotent stem cell markers in the human fetal testis. *Stem Cells* 2008;**26**: 412–421.

Lawson KA, Hage WJ. Clonal analysis of the origin of primordial germ cells in the mouse. *Ciba Found Symp* 1994;**182**:68–84; discussion –91.

Leitch HG, Smith A. The mammalian germline as a pluripotency cycle. *Development* 2013;**140**:2495–2501.

Lengner CJ, Camargo FD, Hochedlinger K, Welstead GG, Zaidi S, Gokhale S, Scholer HR, Tomilin A, Jaenisch R. Oct4 expression is not required for mouse somatic stem cell self-renewal. *Cell Stem Cell* 2007;**1**:403–415.

Li LH, Donald JM, Golub MS. Review on testicular development, structure, function, and regulation in common marmoset. *Birth Defects Res B Dev Reprod Toxicol* 2005;**74**:450–469.

Lin ZY, Imamura M, Sano C, Nakajima R, Suzuki T, Yamadera R, Takehara YOkano HJ, Sasaki E, Okano H. Molecular signatures to define spermatogenic cells in common marmoset (*Callithrix jacchus*). *Reproduction* 2012;**143**:597–609.

Mamsen LS, Brochner CB, Byskov AG, Mollgard K. The migration and loss of human primordial germ stem cells from the hind gut epithelium towards the gonadal ridge. *Int J Dev Biol* 2012;**56**:771–778.

McKay D, Hertig AT, Adams EC, Danziger S. Histochemical observations on the germ cells of human embryos. *Anat Rec* 1953;**117**:201–219.

McKinnell C, Mitchell RT, Walker M, Morris K, Kelnar CJ, Wallace WH, Sharpe RM. Effect of fetal or neonatal exposure to monobutyl phthalate (MBP) on testicular development and function in the marmoset. *Hum Reprod* 2009;**24**:2244–2254.

McKinnell C, Mitchell RT, Morris K, Anderson RA, Kelnar CJ, Wallace WH, Sharpe RM. Perinatal germ cell development and differentiation in the male marmoset (*Callithrix jacchus*): similarities with the human and differences from the rat. *Hum Reprod* 2013;**28**:886–896.

Merker HJ, Sames K, Csato W, Heger W, Neubert D. The embryology of *Callithrix jacchus*. In: Neubert D, Merker HJ, Hendrickx AG (eds). *Non-human Primate: Developmental Biology and Toxicology*. Wien: Ueberreuter Wissenschaft, 1988, 217–242.

Mitchell RT, Cowan G, Morris KD, Anderson RA, Fraser HM, McKenzie KJ, Wallace WH, Kelnar CJ, Saunders PT, Sharpe RM. Germ cell differentiation in the marmoset (*Callithrix jacchus*) during fetal and neonatal life closely parallels that in the human. *Hum Reprod* 2008; **23**:2755–2765.

Mollgard K, Jespersen A, Lutterodt MC, Yding Andersen C, Hoyer PE, Byskov AG. Human primordial germ cells migrate along nerve fibers and Schwann cells from the dorsal hind gut mesentery to the gonadal ridge. *Mol Hum Reprod* 2010;**16**:621–631.

Molyneaux KA, Stallock J, Schaible K, Wylie C. Time-lapse analysis of living mouse germ cell migration. *Dev Biol* 2001;**240**:488–498.

Molyneaux KA, Schaible K, Wylie C. GP130, the shared receptor for the LIF/ IL6 cytokine family in the mouse, is not required for early germ cell differentiation, but is required cell-autonomously in oocytes for ovulation. *Development* 2003;**130**:4287–4294.

Muller T, Fleischmann G, Eildermann K, Matz-Rensing K, Horn PA, Sasaki E, Behr RL. A novel embryonic stem cell line derived from the common marmoset monkey (*Callithrix jacchus*) exhibiting germ cell-like characteristics. *Hum Reprod* 2009;**24**:1359–1372.

Nichols J, Zevnik B, Anastassiadis K, Niwa H, Klewe-Nebenius D, Chambers I, Scholer H, Smith A. Formation of pluripotent stem cells in

the mammalian embryo depends on the POU transcription factor Oct4. *Cell* 1998;**95**:379–391.

Niwa H, Miyazaki J, Smith AG. Quantitative expression of Oct-3/4 defines differentiation, dedifferentiation or self-renewal of ES cells. *Nat Genet* 2000;**24**:372–376.

O'Rahilly R, Muller F. *Human Embryology & Teratology*. 3rd edn. New York: Wiley, 2001.

Pereda J, Zorn T, Soto-Suazo M. Migration of human and mouse primordial germ cells and colonization of the developing ovary: an ultrastructural and cytochemical study. *Microsc Res Tech* 2006;**69**:386–395.

Perrett RM, Turnpenny L, Eckert JJ, O'Shea M, Sonne SB, Cameron IT, Wilson DI, Rajpert-De Meyts E, Hanley NA. The early human germ cell lineage does not express SOX2 during *in vivo* development or upon *in vitro* culture. *Biol Reprod* 2008;**78**:852–858.

Pesce M, Farrace MG, Piacentini M, Dolci S, De Felici M. Stem cell factor and leukemia inhibitory factor promote primordial germ cell survival by suppressing programmed cell death (apoptosis). *Development* 1993; **118**:1089–1094.

Pesce M, Di Carlo A, De Felici M. The c-kit receptor is involved in the adhesion of mouse primordial germ cells to somatic cells in culture. *Mech Dev* 1997;**68**:37–44.

Phillips IR. *The Embryology of the Common Marmoset (*Callithrix jacchus*). Advances in Anatomy, Embryology and Cell Biology*. Berlin-Heidelberg: Springer, 1976.

Politzer G. Die Keimbahn des Menschen. *Z Anat Entwickl Gesch* 1933; **100**:331–361.

Rajpert-De Meyts E, Hanstein R, Jorgensen N, Graem N, Vogt PH, Skakkebaek NE. Developmental expression of POU5F1 (OCT-3/4) in normal and dysgenetic human gonads. *Hum Reprod* 2004;**19**:1338–1344.

Richardson BE, Lehmann R. Mechanisms guiding primordial germ cell migration: strategies from different organisms. *Nat Rev Mol Cell Biol* 2010; **11**:37–49.

Saitou M, Yamaji M. Germ cell specification in mice: signaling, transcription regulation, and epigenetic consequences. *Reproduction* 2010;**139**: 931–942.

Sasaki E, Suemizu H, Shimada A, Hanazawa K, Oiwa R, Kamioka M, Tomioka I, Sotomaru Y, Hirakawa R, Eto T *et al.* Generation of transgenic non-human primates with germline transmission. *Nature* 2009;**459**:523–527.

Shamblott MJ, Axelman J, Wang S, Bugg EM, Littlefield JW, Donovan PJ, Blumenthal PD, Huggins GR, Gearhart JD. Derivation of pluripotent stem cells from cultured human primordial germ cells. *Proc Natl Acad Sci USA* 1998;**95**:13726–13731.

Stallock J, Molyneaux K, Schaible K, Knudson CM, Wylie C. The pro-apoptotic gene Bax is required for the death of ectopic primordial germ cells during their migration in the mouse embryo. *Development* 2003;**130**:6589–6597.

Wang X, Dai J. Concise review: isoforms of OCT4 contribute to the confusing diversity in stem cell biology. *Stem Cells* 2010;**28**:885–893.

Warthemann R, Eildermann K, Debowski K, Behr R. False-positive antibody signals for the pluripotency factor OCT4A (POU5F1) in testis-derived cells may lead to erroneous data and misinterpretations. *Mol Hum Reprod* 2012; **18**:605–612.

West JA, Viswanathan SR, Yabuuchi A, Cunniff K, Takeuchi A, Park IH, Sero JE, Zhu H, Perez-Atayde A, Frazier AL *et al.* A role for Lin28 in primordial germ-cell development and germ-cell malignancy. *Nature* 2009;**460**:909–913.

Witschi E. Migration of the germ cells of human embryo from the yolk sac to the primitive gonadal folds. *Contrib Embryol* Canegie Insitute 1948;**32**:67–97.

Wrobel KH, Suss F. Identification and temporospatial distribution of bovine primordial germ cells prior to gonadal sexual differentiation. *Anat Embryol* 1998;**197**:451–467.

Yeom YI, Fuhrmann G, Ovitt CE, Brehm A, Ohbo K, Gross M, Hubner K, Scholer HR. Germline regulatory element of Oct-4 specific for the totipotent cycle of embryonal cells. *Development* 1996;**122**:881–894.

Yu J, Vodyanik MA, Smuga-Otto K, Antosiewicz-Bourget J, Frane JL, Tian S, Nie J, Jonsdottir GA, Ruotti V, Stewart R *et al.* Induced pluripotent stem cell lines derived from human somatic cells. *Science* 2007;**318**: 1917–1920.

Zwaka TP, Thomson JA. A germ cell origin of embryonic stem cells? *Development* 2005;**132**:227–233.